A TEM and electron energy loss spectroscopy (EELS) investigation of active and inactive silver particles for surface enhanced resonance Raman spectroscopy (SERRS)

Imran Khan,*[a] Dale Cunningham,[b] Sorin Lazar,[c] Duncan Graham,[b] W. Ewen Smith[b] and David W. McComb[a]

Received 12th May 2005, Accepted 6th July 2005
First published as an Advance Article on the web 19th October 2005
DOI: 10.1039/b506644a

A number of silver particles and aggregates of particles were studied using surface enhanced resonance Raman spectroscopy (SERRS), high resolution transmission electron microscopy (HRTEM) and electron energy-loss spectroscopy (EELS). The SERRS mapping/TEM collage method developed previously in our group allows each SERRS active or inactive species to be reliably identified and analysed by each of the techniques in three different instruments. Our aim is to correlate SERRS activity, particle microstructure, chemical composition and electronic properties of each species to gain an insight into the enhancement mechanism. To date, our findings do not reveal any clear link between particle microstructure and SERRS activity. Additionally, the direction of the polarisation of the incident excitation or the presence of interparticle junctions between aggregated particles was not correlated with SERRS activity. However, spectral variations in the EELS data from structurally similar particles and SERRS active and inactive particles suggest that each species is chemically/electronically distinct. Differences in the spectra of single particles, dimers and clusters were also observed. Further analysis of the data, including extraction of the complex dielectric function from the EELS data, will provide an insight into the relationship between these observations and SERRS activity.

Introduction

Surface enhanced resonance Raman spectroscopy (SERRS) is a powerful analytical technique capable of single molecule detection and characterisation.[1,2] Although the general mechanisms of SERRS are broadly accepted,[3,4] the processes occurring at SERRS active sites, where enormous enhancements of the Raman signal occur and single molecule detection is possible, are poorly understood. The analysis of SERRS from analyte molecules adsorbed onto silver particles has been one of the most informative ways of studying the SERRS mechanism and the different systems studied include isolated single particles,[1,5,6] dimers[6–8] and clusters[5,6,9–11] as well as ensemble averaged measurements from thousands of aggregated particles.[2,12] In previous studies we have developed an effective method for the analysis of a statistically significant number of immobilised nanoparticles by both SERRS and transmission electron microscopy (TEM).[5,6] This method involves the correlation of a SERRS map, recorded using an optical microscope, with a collage

[a] *Department of Materials, Imperial College London, London, UK, SW7 2AZ. E-mail: imran.r.khan@imperial.ac.uk*
[b] *Department of Pure and Applied Chemistry, University of Strathclyde, Glasgow, UK, G1 1XL*
[c] *National Centre for High Resolution Electron Microscopy, Kavli Institute of Nanoscience, Delft University of Technology, Delft, The Netherlands*

of TEM images of the same area of the substrate. Recently, we improved this method through the use of fluorescent beads that act as optical markers.[13] Using this method, SERRS active and inactive particles were reliably identified in three different instruments and studied by high resolution transmission electron microscopy (HRTEM) and electron energy-loss spectroscopy (EELS).

EELS is the analysis of the energy distribution of primary electrons that are inelastically scattered upon interaction with the specimen in the TEM. The technique yields a wealth of information concerning the electronic structure, chemical bonding and dielectric response of the specimen atoms.[14] The inelastic events that result in spectral features are primarily electron–electron interactions and include single electron excitations, such as intra- and inter-band transitions and inner-shell ionisations, as well as collective electron oscillations such as the bulk and surface plasmons. The electron energy-loss spectrum can be divided into the valence loss region, which includes energy losses up to 50 eV, and the core loss region where higher energy losses are measured. In this paper, we focus on the valence loss spectrum where intra- and inter-band transitions as well as plasmon excitations occur. The largest feature in each spectrum is the elastic or zero-loss peak (ZLP). The ZLP is associated with the electrons that do not interact inelastically with the sample and the full-width half maximum (FWHM) of the peak provides a measure of the energy resolution of the system. In a modern field-emission gun (FEG) TEM the FWHM of the ZLP is typically ≥ 0.8 eV. If one is interested in features close to the ZLP, *i.e.* $\Delta E < 5$ eV, then removal of the tail of the ZLP is problematic and often results in noise amplification that can mask the features of interest. Key to the success of the EELS measurements in this study is the use of a FEG-TEM fitted with a monochromated source that enables a ZLP with FWHM = 0.1 eV to be formed. This enhanced resolution maximises the chances of resolving and identifying the low energy excitations in the silver particles that could potentially provide insight into the origins of SERRS. It should be noted that in this work a Raman excitation of 514.5 nm was used. It is possible that use of a different excitation wavelength would result in different particles and aggregates being active.

Experimental

Raman spectra were obtained using a Renishaw Raman InVia system in confocal set-up equipped with a Spectra Physics 514.5 Ar^+ laser and Renishaw XYZ mapping stage. With a $\times 100$ objective, the lateral resolution of the Raman system was measured to be approximately 1 μm. The laser power at the sample was measured to be 15 μW. Raman mapping times of approximately 1 hour were employed and under these conditions no photodegradation of the particle–dye complex occurs.[5]

Electron microscopy was performed using a JEOL 2010 TEM, operating at 200 kV, and fitted with a LaB_6 filament. A Gatan Multiscan digital camera was used for image capture. EELS measurements were performed on a FEI Tecnai F20, operating at 200 kV, fitted with a monochromator and a high resolution Gatan Imaging Filter spectrometer.[15] The energy resolution of the system was 0.1 eV. The EELS experiments were performed in image mode such that an image of the specimen was visible on the viewing screen. The spectra were corrected for gain variations on the CCD and the dark current was removed. For each EELS spectrum shown, a series of 25 spectra were collected, aligned and summed.

Silver colloid and the analyte dye 3,5-dimethoxy-4-(5′-azobenzotriazoyl)phenylamine, ABT-DMOPA, were prepared as described previously.[5] Silver colloid was immobilised on labelled SiO_x TEM grids (SPI, Pennsylvania, USA) in a manner similar to that described previously.[5] However, for all experiments detailed here, the grids were not coated with formvar and were not silanised. In brief, each grid was rinsed in methanol, allowed to dry and 1 drop of a dilute colloid was placed on one side of the grid and allowed to evaporate completely. The grid was rinsed in water and then methanol before 1 drop of analyte dye (ABT-DMOPA, 1×10^6 M) was applied to the same side of the grid. After 5 min, the excess dye was washed from the grid by immersion in methanol. A suspension of fluorescent beads in methanol (P.A.R.I.S., Paris, France) was diluted to a suitable concentration, then 1 drop was applied to the same side of the grid. After 5 min, the grid was rinsed in methanol.

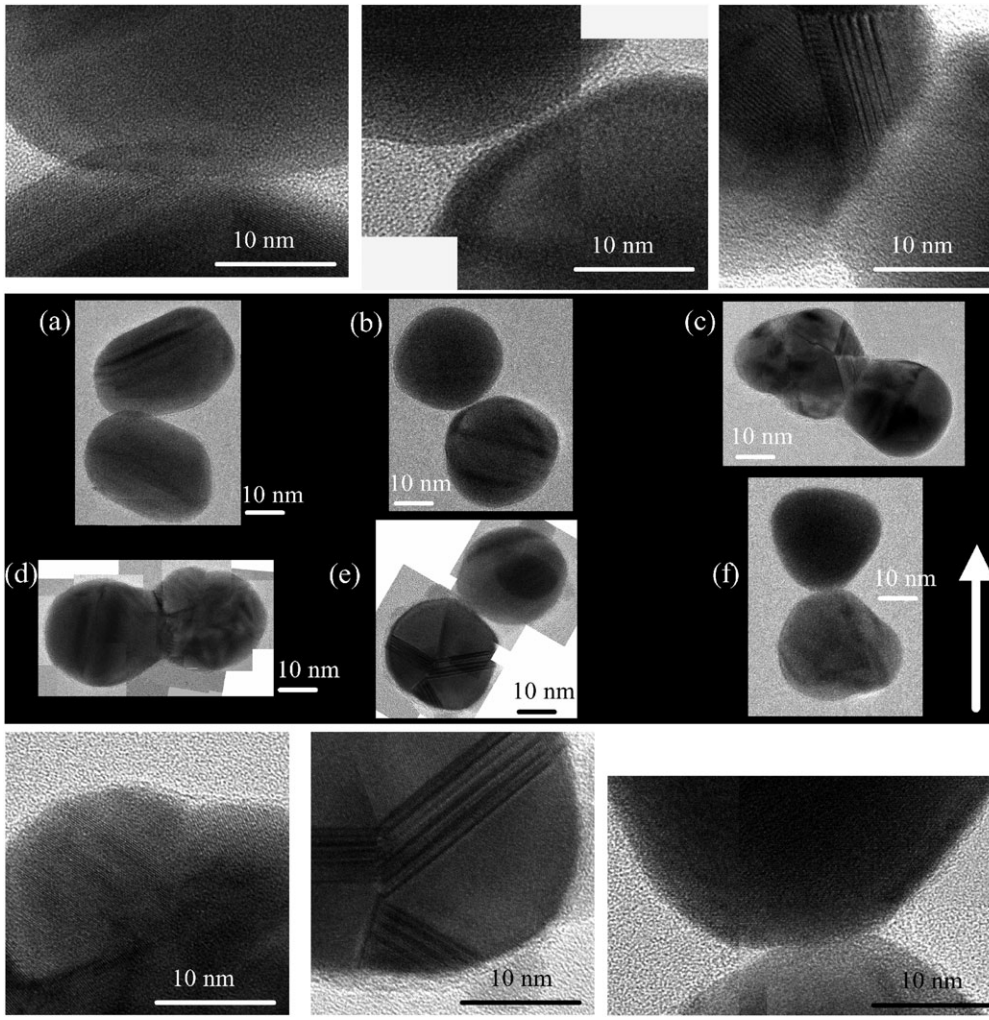

Fig. 1 HRTEM images of SERRS active dimers (a–d) and SERRS inactive dimers (e, f). An enlarged image from a section of each dimer is also shown above (a–c) and below (d–f) the dimer images. The arrow shows the direction of the polarisation of the Raman laser.

Results and discussion

Presented in Fig. 1 are HRTEM images of four SERRS active (a–d) and two SERRS inactive dimers (e,f) each set to the same scale. Each dimer was spatially isolated such that SERRS was collected from the dimer alone without a contribution from any other particle or aggregate of particles. Therefore the SERRS activity can be unambiguously assigned to each of the dimers shown in Fig. 1. A section from each of the dimers is enlarged and shown either above (a–c) or below (d–e) the image of the dimer. In each image silver lattice fringes are visible although the particles were not tilted to orientate a specific zone axis before imaging. Instead, the images show the particles orientated as they were for SERRS analysis. As discussed previously, SERRS activity in dimers may be related to the dimensions of the interparticle junction, orientation relative to the polarisation of the incident light and crystal defects present within the particle.[6] In dimer (b), a gap of approximately 0.5 nm exists between the particles and the dimer is SERRS active. Dimers (e) and (f) are SERRS inactive and the particles in both these dimers are overlapped. These observations support the theory that it is the junction between the particles that is crucial for effective SERRS.

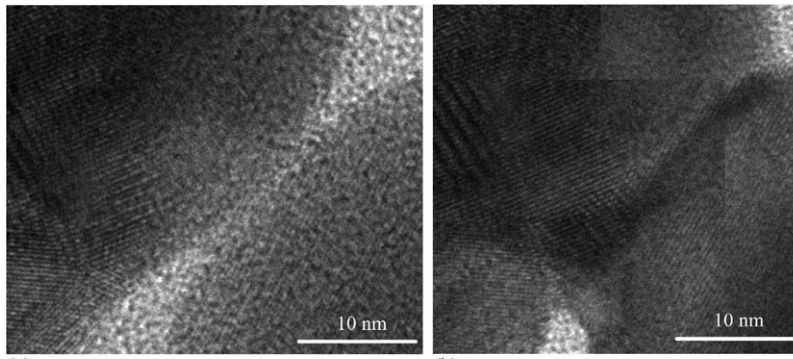

Fig. 2 HRTEM images of the junction between two particles in a dimer (a) before (b) after damage by the electron beam.

However, dimer (a) is also active, yet here the two particles overlap such that the edge of one particle can be seen positioned on top of the other. For each of these dimers, the dimer axis is parallel, or close to parallel, to the polarisation of the incident light. However, in the case of dimers (c) and (d), each of which are SERRS active, the dimer axis lies perpendicular to the direction of the incident polarisation. It would therefore appear that SERRS activity is not dependent on the direction of the incident polarisation relative to the dimer axis. The particles in dimers (c) and (d) appear to be joined together and this will be discussed below. Diffraction contrast features, indicative of crystal defects, are visible in all of the images. The most distinct features occur in dimer (e). The lower particle exhibits a series of dark lines, possibly as a result of twin boundaries, that split the particle into three subcrystals. In the upper subcrystal, the single dark line is indicative of a line defect. The diffraction contrast observed in the enlarged image of dimer (c) may also be indicative of the presence of multiply twin boundaries. It should be noted that the visibility of such contrast is highly sensitive to the orientation of the particles with respect to the electron beam. A detailed electron diffraction study to fully characterise these defects and boundaries is ongoing. As discussed previously, crystal defects present within silver particles could result in high energy sites at the particle surface that may act as SERRS active sites.[6] However, dimer (c) is SERRS active and dimer (e) is SERRS inactive suggesting that these crystal defects do not contribute to effective surface enhancement and do not play a significant role in rendering a particle SERRS active. In addition to our previous findings,[6] these results suggest that there is little evidence for a correlation between high SERRS activity and the presence of a narrow junction or junctions between the particles, crystal defects or the orientation of aggregated particles relative to the incident excitation.

An important consideration when analysing silver nanoparticles by TEM is sample degradation from exposure to the electron beam. The particles in dimers (c) and (d) appear to be joined together in a manner not usually observed and it is believed that this is the result of beam damage. This process is illustrated in a separate study, shown in Fig. 2, where the junction between the two particles in a dimer is shown before and after electron beam damage. In Fig. 2(a) the HRTEM image shows that the edge of each particle is clearly visible. In Fig. 2(b) the particles have melted together and no interparticle junction remains. In this case, particle degradation occurred after approximately 20 min of imaging with the electron beam illuminating the dimer. Particle damage is more prevalent the stronger the electron beam intensity and the older the sample is, *i.e.* the number of days after particle immobilisation.

The lack of a correlation between particle microstructure and SERRS activity motivated our analysis of the electronic properties of SERRS active and inactive silver particles using EELS. The microscope setup utilised a small entrance aperture (0.65 mm) to the spectrometer in order to achieve an energy resolution of approximately 0.1 eV. In this setup however, only a portion of one particle (approximately 10 nm^2) could be sampled. The use of a larger aperture (2 mm) allowed a larger area to be sampled (30 nm^2), but the resolution in this setup was degraded to approximately 0.3 eV. At this resolution much of the detail in the EELS spectra was unresolved. Therefore, the

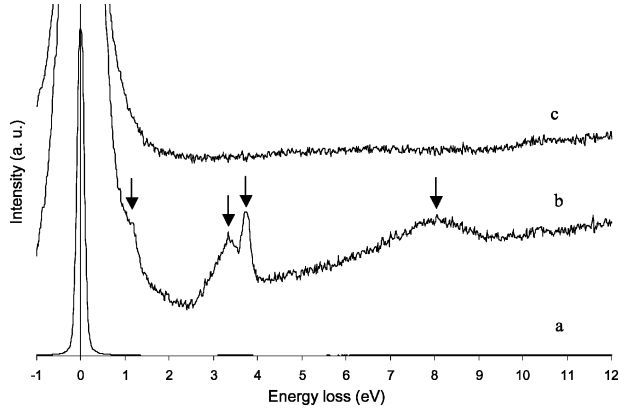

Fig. 3 (a) EELS spectrum from a silver particle. (b) Spectrum expanded by $\times 200$ on the y-axis. (c) EELS spectrum from the SiO_x substrate expanded ($\times 200$). (b) and (c) have been displaced vertically for clarity.

EELS spectra were recorded from an area of each of the particles studied and for aggregated particles the area of the interparticle junction could also be analysed.

Fig. 3(a) shows a typical energy-loss spectrum obtained from a silver particle in this study. As discussed earlier the most intense peak in the spectrum corresponds to the zero-loss peak (ZLP). The spectrum is expanded in Fig. 3(b) to show the detail of the valence loss region. In all subsequent spectra we will omit the zero loss peak. The published data on energy losses from silver systems include the presence of inter-band transitions at 3.3 and 5 eV, a surface plasmon excitation at 3.5 eV and a bulk plasmon excitation at 3.8 eV.[16–18] In Fig. 3 there are two peaks at 3.3 and 3.8 eV and a broad peak at approximately 8.0 eV. There is also a shoulder on the ZLP at 1.2 eV. These features probably correspond with some of the excitations reported in the literature but further analysis of our data is required before assignments can be definitively made. In this energy range there are no features in the spectrum recorded from the SiO_x substrate (Fig. 3c).

In Fig. 4, a comparison of the energy loss spectra recorded from single particles and aggregates of particles are presented. The spectra have been expanded and shifted vertically on the y-axis for

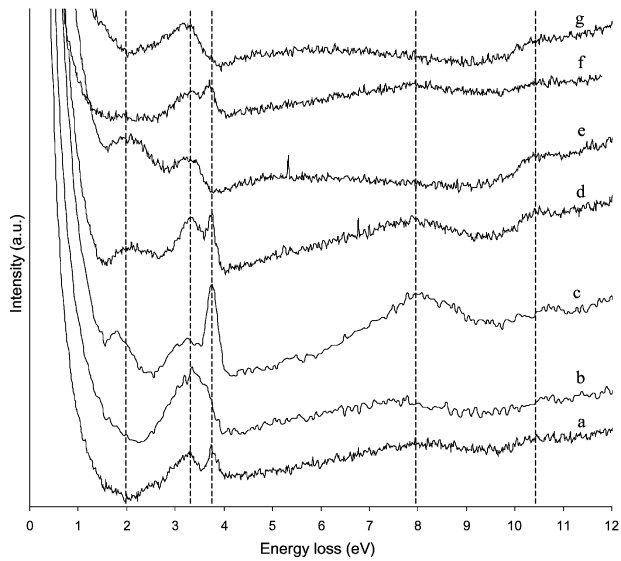

Fig. 4 EELS spectra recorded from (a) single particle (b) dimer junction (c) dimer particle (d) junction between 3 particles in a trimer (e) trimer particle (f) junction between two particles in a quartet (g) quartet particle.

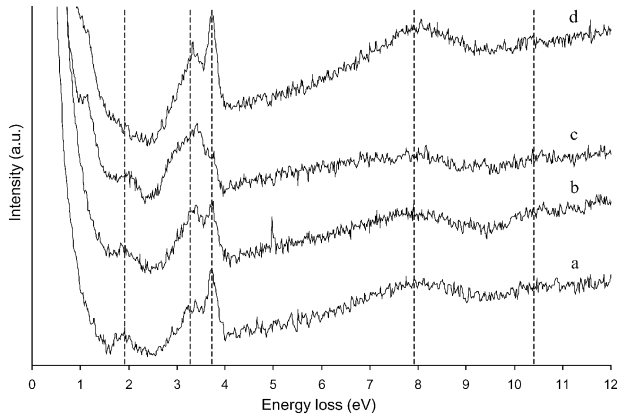

Fig. 5 EELS spectra from a SERRS active dimer (a) particle 1 (b) particle 2 and a SERRS inactive dimer (c) particle 1 (d) particle 2 nm.

clarity. For the aggregates, spectra were recorded from the centre of the particles as well as from the interfaces between the particles. The EELS measurements reveal spectral variations between single and aggregated particles proving that each of the species is chemically and/or electronically distinct. This result is consistent with electromagnetic theory[3,8] where coupling and shifting of surface plasmons occur in aggregated particles relative to the case of an isolated particle. In Fig. 4 there are peaks observed at approximately 2.0, 3.4, 3.8, 8.1 and 10.5 eV and each of these peaks is indicated by dashed lines. The exact position of each of these peaks varies by up to 0.2 eV in the case of some of the spectra. Sharp features are present in the majority of spectra at 3.3 and 3.8 eV although the relative intensities of the peaks vary and the broad bands at approximately 8.1 and 10.5 are less well defined in energy and not present in all spectra. A notable difference between the spectra is the presence of a low energy excitation from aggregated particles. This peak is present at 1.8 eV in the dimer particle and at 2.1 eV in the trimer particle. This trend is not continued for the quartet particle, from which no low energy peak is observed. From studies of a number of dimers, this low energy peak has been observed between 1.8–2.0 eV, although, in some cases the peak is absent. Interestingly, in all cases where the low energy peak is present, it is detected from the particle and not from the junction between particles. If the low energy peak is associated with particle aggregation, its presence would have been expected between particles, where coupling effects are likely to occur. However, a number of single particles were analysed and in no case was the low energy peak observed. A peak in this spectral region has been observed previously, although the authors attributed its presence to imperfections in the silver film.[16]

Comparisons between a number of single particles and dimers reveal that there are also electronic differences between structurally similar particles and aggregates. In Fig. 5, spectra from a SERRS active and an inactive dimer are compared. The relative intensity fluctuations of the 3.3 and 3.8 eV peaks are apparent, as are the slight changes in the position in the broad excitation at approximately 8 eV. The one major difference is the presence of the low energy peak in three out of the four particles, but its absence in one of the inactive particles. One or more of these features may be linked to SERRS activity but it is clear that many more cases must be studied in order to pinpoint spectral features that are unique to SERRS active particles.

Fig. 6 shows a TEM image of a SERRS active quartet of particles. HRTEM images from two of the particles and two of the junctions are also shown together with the associated energy-loss spectra which are recorded from the same area. The SERRS spectrum detected from the quartet is also presented. This figure demonstrates the wealth of information that may be recorded from a silver particle or aggregate of particles through the techniques described in this and other publications.[5,6,13] Particle degradation prevented the analysis of more active/inactive particles by HRTEM with EELS. Ideally, low magnification imaging and assembly of the TEM collage, HRTEM and EELS would be performed in one day, in one TEM, without removal of the specimen from the microscope.

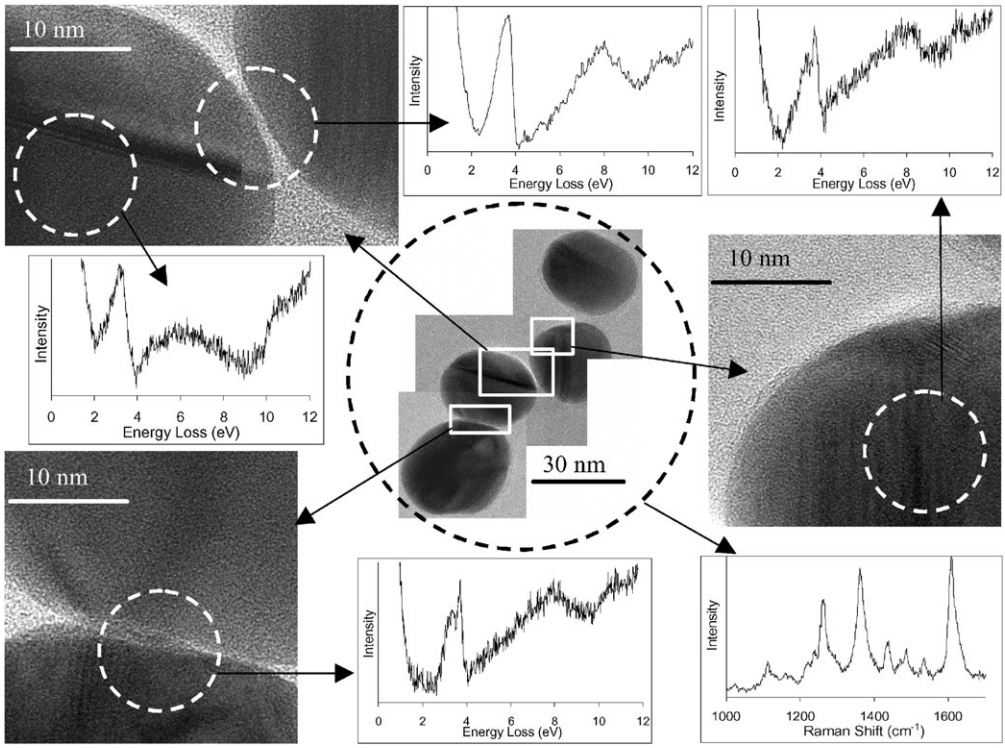

Fig. 6 TEM image of SERRS active cluster of 4 particles. HRTEM images of four regions of the cluster are shown. The EELS spectra shown are recorded from the circled regions. The SERRS spectrum recorded from the cluster is also shown.

A drawback to these experiments is that only a part of a particle may be probed and EELS is not collected from, for example, the dimer as a whole. In future studies it will hopefully be possible to achieve this. In addition, it will be necessary to collate the SERRS spectrum, HRTEM image and EELS spectrum for a number of SERRS active and inactive single particles, dimers and clusters in order to better study and understand the underlying mechanisms of SERRS activity.

Conclusions

The SERRS mapping/TEM collage method allows a significant number of SERRS active and inactive particles to be identified. From these active and inactive particles, both HRTEM images, allowing analysis of particle microstructure, and EELS spectra, allowing plasmon energies and single electron transitions to be measured, may be collected from individual silver particles in the TEM. So far, from all particles assessed, no clear correlation has been observed between particle microstructure and SERRS activity. However, EELS measurements have demonstrated that structurally similar particles exhibit unique chemical properties. Further analysis and derivation of the dielectric constant for these systems may allow these chemical properties to be related to the pronounced differences in SERRS activity exhibited by structurally similar silver particles, dimers and clusters.

The combination of the SERRS spectrum, HRTEM imaging and EELS measurements from identifiable SERRS active and inactive particles should aid a fuller understanding of the underlying SERRS enhancement mechanisms. However, it will be necessary to increase the statistical number of particles studied by the combination of all three techniques before definitive conclusions can be reached.

References

1 S. R. Emory and S. Nie, *Science*, 1997, **275**, 1102.
2 K. Kniepp, Y. Wang, H. Kneipp, L. T. Perelman, I. Itzkan, R. R. Dasari and M. Feld, *Phys. Rev. Lett.*, 1997, **78**, 1667.
3 M. Moscovits, *Rev. Mod. Phys.*, 1985, **57**, 783.
4 A. Campion and P. Kambhampati, *Chem. Soc. Rev.*, 1998, **27**, 241.
5 I. Khan, E. Polwart, D. W. McComb and W. E. Smith, *Analyst*, 2004, **129**, 950.
6 I. Khan, D. Cunningham, D. Graham, D. W. McComb and W. E. Smith, *J. Phys. Chem. B*, 2005, **109**, 3454.
7 H. Xu, E. J. Bjerneld, M. Kall and L. Borjesson, *Phys. Rev. Lett.*, 1999, **83**, 4357.
8 H. Xu, J. Aizpurua, M. Kall and P. Apell, *Phys. Rev. E*, 2000, **62**, 4318.
9 V. A. Markel, V. M. Shalaev, P. Zhnag, W. Huynh, L. Tay, T. L. Haslett and M. Moscovits, *Phys. Rev. B*, 1999, **59**, 10903.
10 A. M. Michaels, M. Nirmal and L. E. Brus, *J. Am. Chem. Soc.*, 1999, **121**, 9932.
11 A. M. Michaels, J. Jiang and L. E. Brus, *J. Phys. Chem. B*, 2000, **104**, 11965.
12 P. Hildebrandt and M. Stockburger, *J. Phys. Chem.*, 1984, **88**, 5935.
13 I. Khan, D. Cunningham, R. E. Littleford, D. Graham, W. E. Smith and D. W. McComb, *Anal. Chem.*, 2006, **78**, 224.
14 R. F. Egerton, *Electron Energy Loss Spectroscopy in the Electron Microscope*, Plenum Press, New York, 2nd edn., 1996.
15 D. S. Su, H. W. Zandbergen, P. C. Tiemeijer, G. Kothleitner, M. Havecker, C. Hebert, A. Knop-Gericke, B. H. Freitag, F. Hofer and R. Schlogl, *Micron*, 2003, **34**, 235.
16 C. J. Flaten and E. A. Stern, *Phys. Rev. B*, 1975, **11**, 638.
17 A. Yelon, K. N. Piyakis and E. Sacher, *Surf. Sci.*, 2004, **569**, 47.
18 F. Ouyang, P. E. Batson and M. Isaacson, *Phys. Rev. B*, 1992, **46**, 15421.

